



Vibration Attenuation of Panel Structures by Optimally Shaped Viscoelastic Coating with Added Weight Considerations

L. Cheng & R. Lapointe

Department of Mechanical Engineering, Université Laval, Québec,
Canada G1K 7P4

(Received 5 March 1994; accepted 9 May 1994)

ABSTRACT

This paper presents a study on vibration damping by means of partial viscoelastic coating applied to the surface of vibrating panels. An optimization procedure seeking the location as well as the shape of coverage giving the best damping performance for a given weight of material is established. Emphasis is also put on the temperature and frequency dependent characteristics of the viscoelastic material. The results show the effects of the operating temperature and the great potential of using optimized partial coverage, either to reduce the weight while maintaining the same damping level or to increase the performance with the same amount of material.

INTRODUCTION

Viscoelastic coating damping treatment is widely used in the vibration control of various types of thin-walled structures. When exposed to vibrations, the high polymeric molecular properties exhibited by these materials enhance the system damping, thereby realizing considerable dissipation of vibration energy. Viscoelastic coating is usually used in two ways: constrained and unconstrained layer configuration. The first one, also referred to as sandwich treatment, consists of applying the damping material between the surface of the structure to control and a thin metallic

facing. This type of configuration presents the advantage of being more effective due to the shear deformation caused by the relative movement of the two elastic layers. However, the presence of the constraining layer results in a more considerable added mass to the system. Therefore, unconstrained layer is preferred in many practical situations in which the added weight has to be limited.

Considerable efforts have been made in the past to study the general use of the damping treatment, which can be seen by the substantial amount of published papers on the subject. The earliest work performed in the 1960's permitted a general understanding of such applications to vibration and noise control problems.¹⁻³ A good summary can be found in a review paper by Nakra.⁴ With respect to the full coverage, partial coverage was investigated to a lesser degree. In many practical applications, such as aeronautic and space structures, damping treatment is subject to a very careful consideration of weight economy. Since the partial coverage technique has the advantage of adding less weight, efforts should therefore be made to find its optimal use. Most of the work on partial coverage investigated one-dimensional structures. Among the earliest papers published on the subject, one can cite the ones written by Mead *et al.*,⁵⁻⁶ in which the effects of an unconstrained layer on the fundamental modes have been reported. Since then, one-dimensional structures have been the subject for many researchers and practitioners.⁷⁻¹⁰ As far as partial coverage on two dimensional plane structures is concerned, much less information is available. Parthasarathy investigated the subject with a rectangular plate¹¹ where several coverage configurations are compared in terms of increase of the modal damping factors. The same scenario was later taken by the same author for a rectangular plate having central cutouts.¹² From these works, one got a good understanding of the coverage position although no automatic optimization procedure was used. In fact, from an optimization point of view, not only the optimal position of the coverage should be determined but also the shape to get the optimal damping performance. To our knowledge, no work was reported in the literature to tackle this problem.

Another important aspect related to viscoelastic materials is the operating temperature. As we know, the damping properties of these materials are very sensitive to temperature variations and, to a certain degree, to frequency variations.¹³ For aeronautic and aerospace applications, structures are always exposed to a wide range of temperature. For example, a satellite panel may undergo a temperature range varying from -100°C to $+100^{\circ}\text{C}$ from nights to days. This can considerably affect the mechanical properties of the viscoelastic materials and consequently, the control performance. In this context, although great efforts have been made by

chemical workers to study the dependence of these materials' property under temperature–frequency variations, no sufficient details are available in the literature to illustrate its practical influence from the point of view of mechanical engineering. In fact, the majority of work reported used constant material parameters.^{14–16} For the above-mentioned areas of application, it seems that an optimization algorithm should take these factors into account.

In this paper, we propose a systematic study of the aforementioned issues with a panel structure partially covered by unconstrained layers. A general formulation with an integrated optimization algorithm is established. With respect to the existing literature, this work aims to contribute in the following aspects: (1) With the criteria imposed on the additional weight, the optimization procedure gives the best coating configuration, including the location and the shape, and this either for the modal damping factors or for the structure's response when subjected to a mechanical excitation over a given frequency band. (2) The formulation takes into account the real materials' properties under frequency–temperature variations. (3) Thanks to the mounting conditions modeling of the panel by means of artificial springs, the formulation is capable of handling a wide variety of fixing conditions that may be encountered in practice.

FORMULATION AND RESOLUTION METHOD

Modeling of the system

The investigated structure is a rectangular thin plate (dimensions $2b$, $2h$, $2e$) symmetrically covered on both sides by a certain number of thin unconstrained rectangular pieces of viscoelastic material (see Fig. 1a). The mounting conditions are simulated by a set of translational and rotational springs connecting the plate along its edges to a fixed foundation. As shown in Fig. 1b, these springs are continuously distributed along the edges with various stiffness for each one (k_i in N/m^2 for translation and c_i in N/rad for rotation, $i = 1, 2, 3, 4$). This technique allows the representation of a wide variety of attaching conditions by simply adjusting the stiffness level of the springs.^{17–18} For example, simply supported boundaries can be obtained by giving a high value to the translational springs and a value of zero to the rotational ones. The physical properties of both the plate and the viscoelastic material are assumed to be homogeneous. The own internal damping of the plate is introduced into the model and the temperature–frequency dependent stiffness and loss factor of the viscoelastic material are also taken into consideration.

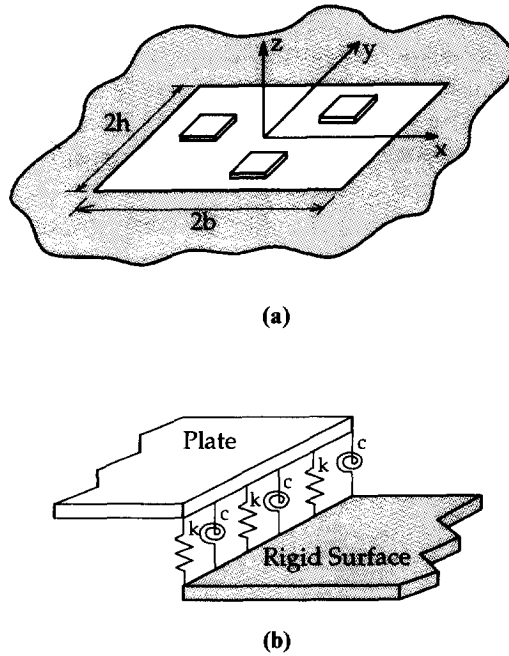


Fig. 1. (a) Representation of the system; (b) modeling of the mounting conditions.

It is well known that shear effects for unconstrained layers are secondary with respect to tension–compression ones. For a thin plate symmetrically coated on both sides, the Love–Kirchoff theory is therefore used as a displacement field for the model:

$$\{u, v, w\} = \left\{ -z \frac{\partial w}{\partial x}, -z \frac{\partial w}{\partial y}, w(x, y, t) \right\} \quad (1)$$

Here the vector $\{u, v, w\}$ represents the displacement of a point either on the plate or on the viscoelastic layer. The flexural displacement w , which has now become the only independent variable, is then approximated by a polynomial expansion over x and y :

$$w(x, y, z) = \sum_{i=0}^m \sum_{j=0}^n \bar{a}_{ij}(t) \left(\frac{x}{b}\right)^i \left(\frac{y}{h}\right)^j \quad (2)$$

where the factors $\bar{a}_{ij}(t)$ are complex and functions of time t . The Lagrange's equations can then be applied to find the stationary state of the system with the factors $\bar{a}_{ij}(t)$ as generalized coordinates:

$$\frac{d}{dt} \left(\frac{\partial L}{\partial \dot{\bar{a}}_{pq}(t)} \right) - \frac{\partial L}{\partial \bar{a}_{pq}(t)} = 0 \quad (p = 0, 1, 2, \dots, m \text{ and } q = 0, 1, 2, \dots, n) \quad (3)$$

where L is the Lagrangian of the system expressed as:

$$L = E_k - E_p + W \quad (4)$$

Here, E_k represents the kinetic energy of the system, E_p the potential energy and W , the work done by the external forces. These terms are given by:

$$E_k = \frac{1}{2} \int_V \rho \left(\frac{\partial w}{\partial t} \right)^2 dV \quad (5)$$

$$\begin{aligned} E_p = & \frac{1}{2} \int_V \frac{E(f, T)z^2}{2(1+\nu)} \left\{ \frac{1}{(1-\nu)} \left[\left(\frac{\partial^2 w}{\partial x^2} \right)^2 + \left(\frac{\partial^2 w}{\partial y^2} \right)^2 + 2\nu \frac{\partial^2 w}{\partial x^2} \frac{\partial^2 w}{\partial y^2} \right] \right. \\ & \left. + 2 \left(\frac{\partial^2 w}{\partial x \partial y} \right)^2 \right\} dV \\ & + \frac{1}{2} \int_{-h}^h \left\{ k_1 [w(-b, y, t)]^2 + k_2 [w(b, y, t)]^2 + c_1 \left[\frac{\partial w(-b, y, t)}{\partial x} \right]^2 \right. \\ & \left. + c_2 \left[\frac{\partial w(b, y, t)}{\partial x} \right]^2 \right\} dy \\ & + \frac{1}{2} \int_{-b}^b \left\{ k_3 [w(x, -h, t)]^2 + k_4 [w(x, h, t)]^2 + c_3 \left[\frac{\partial w(x, -h, t)}{\partial y} \right]^2 \right. \\ & \left. + c_4 \left[\frac{\partial w(x, h, t)}{\partial y} \right]^2 \right\} dx \end{aligned} \quad (6)$$

$$W = \sum_{\delta=1}^{\Delta} [\bar{f}_{\delta}(t) \cdot w(x_{\delta}, y_{\delta}, t)] \quad (7)$$

The symbol Δ in eqn (7) represents the number of forces applied to the system and $(x_{\delta}, y_{\delta}, t)$ the application point of each of them. It should be pointed out that the volume integration described in eqns (5) and (6) should be carried out for both the plate and the viscoelastic layer. Consequently, the corresponding material properties (modulus E , density ρ and Poisson's ratio ν) should be used in due case. The application of the eqns (3) yields a classic $m \times n$ degree of freedom system of linear equations:

$$[M]\{\ddot{\bar{a}}(t)\} + [\bar{K}]\{\bar{a}(t)\} = \{\bar{f}(t)\} \quad (8)$$

in which $[M]$ and $[\bar{K}]$ are, respectively, the mass matrix (real) and stiffness matrix (complex due to the frequency and temperature dependent characteristics of the viscoelastic material). For harmonic excitations the vector of the force and the vector of the response are represented in the following way:

$$\{\bar{f}(t)\} = \{F\} e^{j\omega t} \quad (9)$$

$$\{\bar{a}(t)\} = \{\bar{A}\} e^{j\omega t} \quad (10)$$

which reduce eqn (8) to:

$$[[\bar{K}] - \omega^2[M]]\{\bar{A}\} = \{F\} \quad (11)$$

The formulas for calculating the terms of the matrices and the force vector are given in Appendix 1.

As to the modeling of the stiffness and the damping of viscoelastic materials, substantial research has been done in the past. Among others, Nashiff¹⁹ presented a data base for different kinds of materials via measurements. Several curve-fitting formulas were also developed in the literature. In the present work, the formulas²⁰ for the viscoelastic layer of Soundcoat D made by SOUNDCOAT were used for illustrative purposes. These formulas give the Young's modulus and the loss factor of the material as a function of temperature and frequency. The details are given in Appendix 2.

Resolution of the system

In the present study, both the free and the forced vibration of the structure will be treated. For the case of forced vibrations, eqn (11) should be resolved. For a given temperature and frequency, the corresponding stiffness and damping characteristics of the viscoelastic material are calculated and inserted into the stiffness matrix. The resolution is then made using standard numerical procedures.²¹ The accuracy of the result depends mainly on the truncation of the series used in eqn (2), a compromise has to be found between using high values for m and n (giving great precision and high calculation costs) and low values (giving little precision and low calculation costs). Note that the first modes region do not require high values to give a good precision but the higher ones do.

For the free vibration analysis, the natural frequencies and the corresponding loss factors of the system are found by calculating the eigenvalues of the following equation:

$$[[M]^{-1}[\bar{K}]]\{\bar{A}\} = \omega^2\{\bar{A}\} \quad (12)$$

which is directly taken from eqn (11). The system matrix being temperature and frequency dependent, it requires an iterative procedure to obtain the natural frequencies. For each mode, an initial guess is made (the natural frequency of the undamped plate is a good start) and the calculation is carried out with the corresponding stiffness terms. The value obtained by resolving eqn (12) is then used as a guess for the next iteration. Convergence is obtained in a few steps. The system being complex, the eigenvalues will then have the form:

$$\omega^2 = \omega_n^2(1 + j\eta) \quad (13)$$

where ω_n represents the natural frequency and η the corresponding modal loss factor of the system.

Optimization process

The optimization of the damping performance of the coating is the main issue to be addressed in the present paper. To define the coverage configuration, the plate is first divided into a certain number of small sections (X and Y sections along the x and y axis, respectively). Then, the components of a configuration vector $c(i, j)$ are assigned a value of 1 or 0, depending whether the corresponding section (i, j) is covered or not (see Fig. 2). To find the optimal configuration, an optimization algorithm is developed. Figure 3 shows the main steps of the algorithm. With a pre-determined percentage of the plate to cover and a fixed thickness of viscoelastic material, it starts off with a randomly chosen initial configuration and calculates the objective function, which can be either the modal damping factors or the response. Then it makes a slight change in the configuration and compares the objective function with the previous one. If the result is better, the new configuration is kept. Otherwise, another change is made starting from the previous configuration. This routine is repeated until no noticeable improvement of the performance is encountered after a certain number of steps. A verification of the convergence of the solution has been

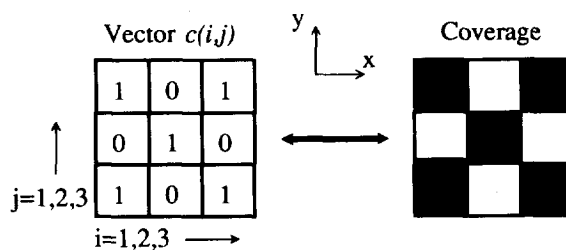


Fig. 2. Representation of the configuration vector.

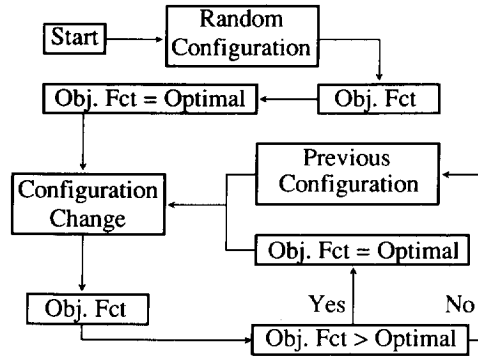


Fig. 3. Optimization algorithm.

carefully made during the calculations to make sure that a global optimal solution was obtained. This way, the calculation gives the optimal location as well as the optimal shape in each case.

EXPERIMENTAL VERIFICATION

To verify the accuracy of the model, an experimental test has been made on an aluminum plate (200 mm by 480 mm by 3.175 mm), as illustrated in Fig. 4. To simulate a free boundary condition, the plate was fixed by four rubber bands of very weak stiffness at the plate's border to a stiff steel frame. The EAR SD-40 viscoelastic material layer was used to cover the plate and a total number of six pieces of 60 mm by 140 mm by 0.040 mm was used. Figure 4 shows the details of the coating.

A shaker was used to apply an external force to the system. The measurement of the force was made by a force transducer placed right between the shaker and the plate via a properly chosen thin rod to avoid any possible moment excitation. The response was given by an accel-

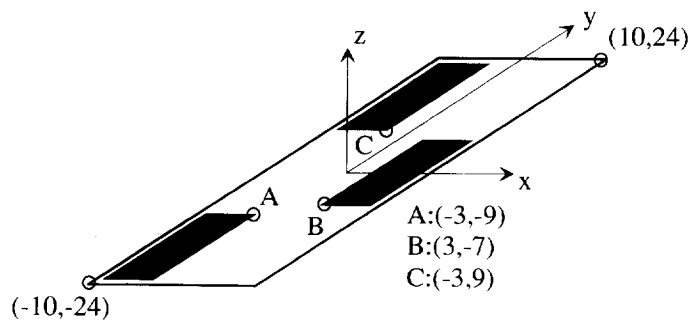


Fig. 4. Coverage used in experimental test.

TABLE 1
Comparison Between Theory and Experiment

| Mode | Undamped plate | | Damped plate | | | |
|------|---------------------------|---------------------------------|---------------------------|--------|---------------------------------|--------|
| | Theory ω_n (Hz) | Experimental ω_n (Hz) | Theory ω_n (Hz) | η | Experimental ω_n (Hz) | η |
| 4 | 72.5 | 72.4 | 70.7 | 0.0220 | 70.25 | 0.0202 |
| 5 | 107.2 | 106.4 | 103.6 | 0.0224 | 101.75 | 0.0207 |
| 6 | 201.5 | 201.6 | 198.3 | 0.0259 | 196.5 | 0.0246 |
| 7 | 230.9 | 229.6 | 225.4 | 0.0283 | 221.75 | 0.0338 |
| 8 | 388.1 | — | 382.2 | 0.0299 | — | — |
| 9 | 389.9 | — | 386.3 | 0.0321 | — | — |
| 10 | 441.1 | 450.2 | 437.9 | 0.0190 | 442.5 | 0.0174 |
| 11 | 481.0 | 484.8 | 479.7 | 0.0208 | 476.3 | 0.0205 |
| 12 | 593.6 | 594.5 | 586.0 | 0.0329 | 574.25 | 0.0352 |

erometer placed on the surface of the plate. Both signals were then sent to an HP-35660 spectral analyzer. The frequency response of the system under a random excitation (white noise) was used to measure the natural frequencies while the damping was measured using the half-power method (-3 dB) with sinusoidal excitations. The results were computed using the SMS-STAR software and they are presented in Table 1.

Since the damping of the aluminum is negligible, only the natural frequencies were measured for the undamped plate. For the damped system, both natural frequencies and the corresponding loss factors are compared. Satisfying results were obtained for the undamped case, as well as for the damped case. In fact, not only did the theory predict the same trend of variation as the experiment, but also the error between the theory and the experiment for both the natural frequencies and the modal damping factors stays within a very satisfactory range. Note that the modes 8 and 9 were very close to one another. No special effort was made during the experiment to identify them. Nevertheless, by the comparison carried out with the rest of the modes, it is concluded that the developed model is accurate enough to ascertain the validity of the simulations.

NUMERICAL RESULTS AND DISCUSSIONS

The characteristics of the plate (aluminum) and the damping material (Soundcoat-D) that were used for the numerical analysis are presented in Table 2 and Appendix 2. For illustrative purposes, a simply supported rectangular plate has been chosen. The main factor leading to this choice was its easiness for visualizing the physical phenomena. For the bare plate,

TABLE 2
Characteristics of the Plate

| <i>Plate (Aluminum)</i> <i>Dimensions and physical properties</i> | |
|--|---------------------------|
| Width ($2b$) | 0.3 [m] |
| Length ($2h$) | 0.45 [m] |
| Thickness ($2e$) | 0.003175 [m] |
| Density (ρ_p) | 2700 [kg/m ³] |
| Young's modulus (E_p) | 70×10^9 [Pa] |
| Loss factor (γ_p) | 0.01 |

a structural damping model with constant damping factor (0.01) was used in all calculations. In each studied case, both the free and the forced vibration are addressed.

General effects of the viscoelastic coatings

To show the general trend of the damped system, Fig. 5 compares the response of the bare plate to that of the same plate but covered entirely by two layers of 1/16" thick viscoelastic material (on both sides) for a room temperature ($T = 20^\circ\text{C}$). A harmonic driving force of 1 N ranging from 0 Hz to 1200 Hz was applied at $x = 3.4$ cm and $y = 8.7$ cm on the plate (the coordinate system having its origin at the center of the plate). From this figure the effects of the coating can be clearly identified. With respect to the bare plate, two main effects are noticed. First, the resonance peaks of the damped system are shifted to lower frequencies in this case due to

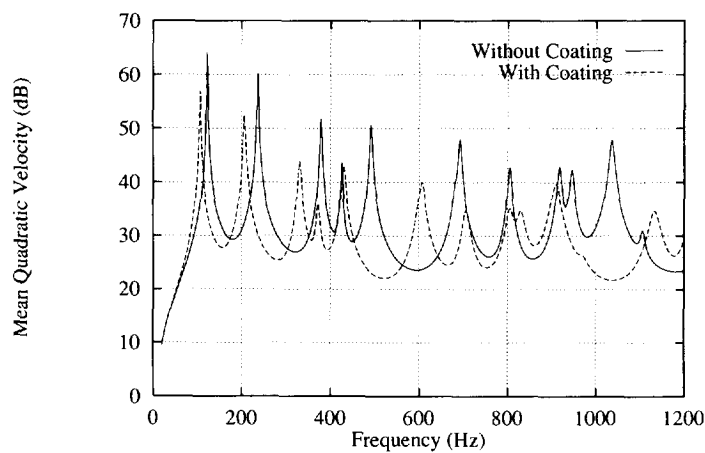







Fig. 5. Effect of 1/16" thick full coverage on the response.

the dominated added mass over the stiffness. Second, vibration levels are reduced, particularly in the vicinity of the resonance due to the increase of the effective damping of the system.

Coatings with optimization

Table 3 shows the effect of various coating configurations on the natural frequency and the damping factor of the first five modes ($T = 20^{\circ}\text{C}$). Note that the same amount of material was used for each configuration of coverage (leading to an added weight of 18% with respect to the bare plate, which means a thickness of $1/32''$ for the full coverage and $1/8''$ for the 1/4 coverage). For the full coverage, as the frequency gets higher, the effect of the viscoelastic material on the damping level is easily seen by the increase of the damping factors. It is worth mentioning that the 1/4 coverage performs generally better than the full coverage and that, without even optimizing the configuration. This is mainly due to the thickness increase of the 1/4 coating layers. However, best results are obtained when the optimization routine is applied to the partial coverage. This can be easily seen by comparing the last two columns. In the last column, the optimal 1/4 coverage is given for each mode with their corresponding natural frequency and damping factor. By engaging the optimization process, one obtains the optimal locations with the associated shapes. For the five modes presented in the table, the increase of damping compared to the full coverage ranges

TABLE 3
Effect of the Coverage on the Modes

| Mode | Uncovered plate | | Full coverage | | 1/4 Coverage | | Optimal 1/4 coverage | | Configuration |
|------|-----------------|---------|-----------------|---------|-----------------|---------|----------------------|---------|---|
| | ω_n (Hz) | η | ω_n (Hz) | η | ω_n (Hz) | η | ω_n (Hz) | η | |
| 1 | 123.3 | 0.01000 | 114.2 | 0.01350 | 114.9 | 0.02067 | 103.9 | 0.02758 |  |
| 2 | 236.9 | 0.01000 | 219.7 | 0.01373 | 223.5 | 0.02051 | 200.5 | 0.02801 |  |
| 3 | 379.1 | 0.01000 | 353.0 | 0.01386 | 360.6 | 0.02093 | 325.5 | 0.03438 |  |
| 4 | 426.2 | 0.01000 | 395.9 | 0.01388 | 399.3 | 0.02274 | 363.1 | 0.03118 |  |
| 5 | 492.5 | 0.01000 | 458.5 | 0.01391 | 475.0 | 0.01725 | 421.0 | 0.02949 |  |










from 2.12 to 2.48. Compared to the non-optimized 1/4 coverage, a noticeable damping increase is also obtained for all the modes considered. It should also be mentioned that the obtained optimal configurations are consistent with the commonly used rules of applying the layers at the antinodal portion of the structure. Moreover, the results indicate that the obtained optimal shapes are more or less ellipse-like.

The same analysis has been made for the response of the plate over different frequency bands. A sinusoidal force of 1 N is still applied at (3.4 cm, 8.7 cm) and for each frequency, the mean quadratic velocity is calculated ($T = 20^\circ\text{C}$). The area under the curve of the mean quadratic velocity (calculated numerically with the frequency on the x -axis) is used as a way of measuring the energy level within a given band. The "Gain" used is defined as follow:

$$\text{Gain} = \frac{\text{Undamped Level} - \text{Damped Level}}{\text{Undamped Level}} \times 100\% \quad (14)$$

Table 4 shows the results for three different frequency bands: 50 Hz–300 Hz (covering the first two modes), 300 Hz–550 Hz (covering the modes 3, 4, 5) and 550 Hz–800 Hz (covering the modes 6, 7 and 8). For each frequency band of interest, the last column of the table gives the optimal configuration. Again the 1/4 coverage shows itself more effective than the full coverage. The optimization process enhances even more the damping performance, reaching a damping increase varying from 78.0% to 88.3% compared to the bare plate, which is approximately twice the performance of the full coverage and about 50% higher than the non-optimized ones. It is interesting to note that, depending on the dominating

TABLE 4
Effect of the Coverage on the Response

| Frequency band (Hz) | Gain (Undamped plate as reference) | | |
|------------------------|--|--|---|
| | Full coverage | 1/4 coverage | Optimized 1/4 coverage |
| 50 - 300 (Hz) |  42.8% |  59.7% |  78.0% |
| 300 - 550 (Hz) |  44.0% |  49.4% |  88.3% |
| 550 - 800 (Hz) |  31.3% |  55.6% |  86.9% |

mode involved for each frequency band and on the location of the exciting force, the obtained optimal arrangement is a combination of the ones previously obtained for each single mode.

It is worth noting that careful convergence verification was made during each optimization calculation to make sure that the final result was a global optimum. It was observed that the developed algorithm permitted a rather rapid convergence and the calculations were carried out within a reasonable time. To illustrate the convergence issue, a typical result is given in Figs 6a and 6b to show the evolution of the gain and the configuration for the 50 Hz–300 Hz band. Starting from a randomly chosen initial configuration, the result converges gradually towards the one that gives the best result. Most of the improvement is made in the first half of the process. In the second half, no significant amelioration of the coverage is made even if the configuration undergoes visible changes.

Temperature effects

To show the effect of the temperature on the modal damping performance of the viscoelastic coatings, the damping factor of the first mode has been calculated for three typical temperatures. The results are presented in Table 5 for -50°C , 20°C and 100°C (the thickness of the coverage is $1/8''$ for both configurations). Note that the damping materials used give maximal loss modulus around 10°C . Therefore it is not surprising to see that, for both coating configurations specified in the first column, stronger damping is obtained at 20°C among the three investigated temperatures. However, a comparison between the two configurations allows one to realize the effects of temperature variation on the optimized results. In fact, the first configuration is the optimal result at -50°C , a temperature at which the damping factor of the viscoelastic material is smaller than the damping that has been assigned to the aluminum. The second one corresponds to the configuration generated by the optimization routine at 20°C , a temperature at which the viscoelastic material is much more dissipating than the bare plate. Therefore, at -50°C , the optimized result indicates that the coverage is made in such a way that the viscoelastic layers interfere as little as possible with the deformation of the structure to be covered. However, when the temperature rises above the critical point of equal damping coefficients, which is the case at 20°C , the damping material should be applied at the anti-nodal portion of the structure. With these two temperatures, the forced responses of the corresponding optimal configurations are plotted in Fig. 7. It can be seen that temperature is an important parameter to consider for predicting precisely the dynamic behavior of the damped system.

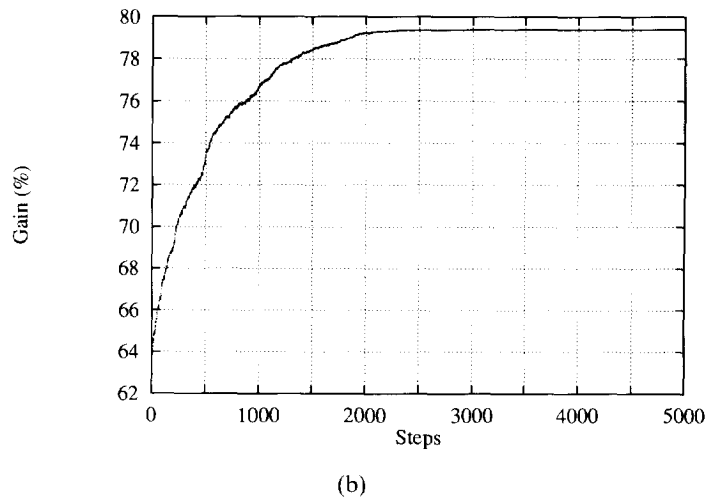
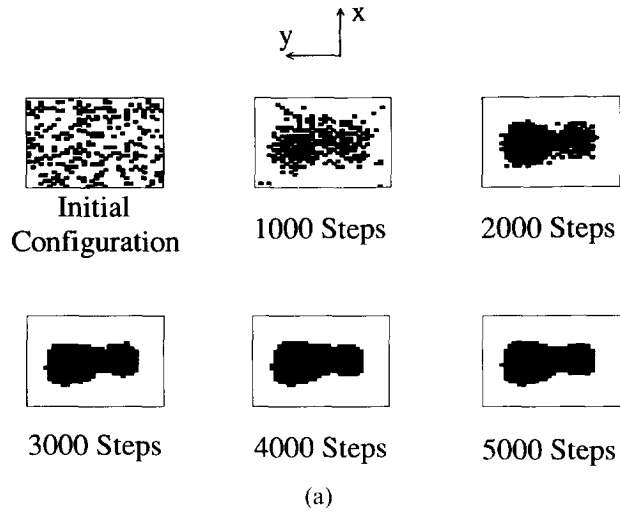
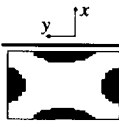



Fig. 6. (a) Evolution of the configuration; (b) evolution of the gain.

Optimization with added weight consideration

This section is intended to show two important issues: firstly, with a certain allowable added weight, how the optimized partial coating may improve the damping performance or inversely, how to get the same damping performance by keeping the added weight minimal. To answer these questions, Fig. 8 compares three configurations: full coverage, non-optimized 1/4 coverage and optimized 1/4 coverage. To better illustrate the additional weight to the structure, the mean quadratic velocity is

TABLE 5
Effect of the Temperature on the Modes

| | $T=-50^{\circ}\text{C}$ | $T=20^{\circ}\text{C}$ | $T=100^{\circ}\text{C}$ |
|---|---|---|---|
|  | $\omega_n = 123.2 \text{ Hz}$ $\eta = 0.00980$ | $\omega_n = 121.6 \text{ Hz}$ $\eta = 0.01299$ | $\omega_n = 121.1 \text{ Hz}$ $\eta = 0.01001$ |
|  | $\omega_n = 112.1 \text{ Hz}$ $\eta = 0.00888$ | $\omega_n = 103.9 \text{ Hz}$ $\eta = 0.02758$ | $\omega_n = 101.2 \text{ Hz}$ $\eta = 0.01007$ |

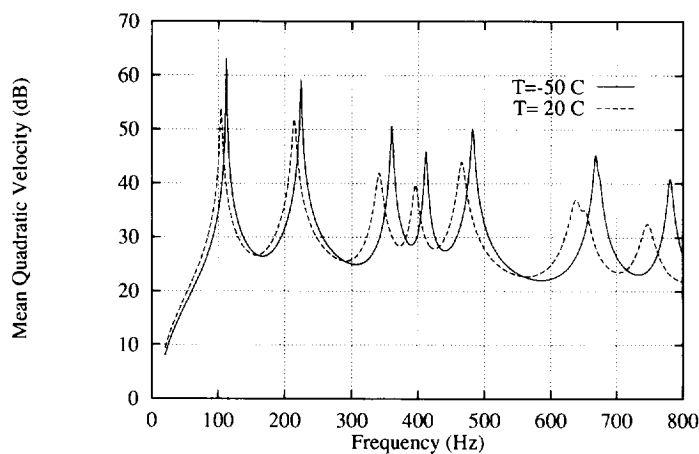


Fig. 7. Effect of the temperature on the response.

expressed as a function of the percentage of weight added (the weight of the plate alone is used as the reference). Note that the thickness of the viscoelastic layers are different depending on the coverage configurations to keep the same added weight. Also, the maximal thickness of the coverage is limited to $1/8''$ (the thickness of the plate). The reason is that our model has been made with the assumption of thin structures. Therefore, the results obtained in this range of thickness can be considered as sufficiently accurate. The frequency band of interest is the 50 Hz–300 Hz with the same external force as the one specified previously. It can be observed that for the same weight added, the 1/4 coverage shows a greater effect on the damping increase than the full coverage. In fact, at the maximum thickness, the gain of the 1/4 coverage (without optimization) is about 1.4 times higher than the one obtained with the full coverage. However, more interesting results are obtained with the optimized 1/4 coverage. For the same amount of viscoelastic material, the 1/4 coverage with optimal shape reaches a reduction of 78% while the full coverage gives only a reduction

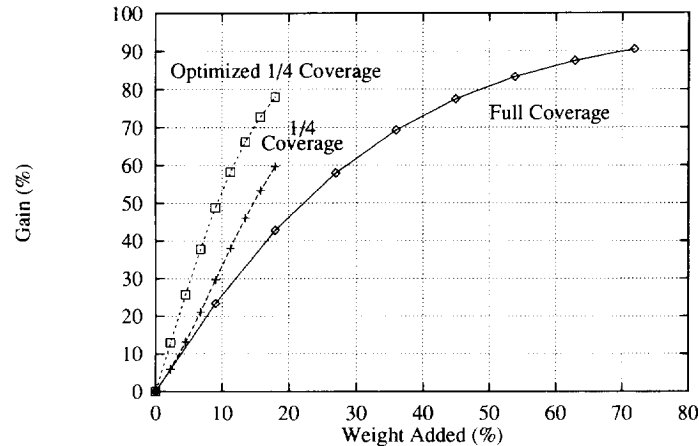


Fig. 8. Effect of the added weight on the response.

of 42%. To get the same reduction level, the full coverage requires an addition of weight of 45%, compared to 18% for the quarter coverage. The non-optimized 1/4 coverage gives intermediate performance. It should be stressed that the gain used here is for a relatively large frequency band. If the excitation has a pure tone or a narrow band, the optimization certainly gives a more appreciable damping improvement.

CONCLUSIONS

The concept of optimal damping with weight constraints using partial coverage on a panel structure has been presented and an application on a simply supported plate has been described. Experimental studies show the validation of the established formulation. The analytical procedure demonstrates its merits in several aspects with respect to the existing literature: capacity of taking into account the real frequency–temperature dependent characteristics of the viscoelastic materials, the generality of the modeling of the boundary conditions of the structures and most importantly, the search for the optimal coating shapes. Numerical studies indicate that, with the cost or the weight of the damping treatment kept constant, partial arrangement with optimal cutting shapes significantly increases the damping performance of the system. Moreover, the operating temperature is a crucial parameter to consider at the design stage for the fields of application where the structures are subject to a wide range of temperature variations. It is concluded that shape optimization with temperature consideration are worth considering in many practical situations.

REFERENCES

1. Oberst, H., Vibration damping of metal structures, especially by optimized amorphous high polymers. In *Amortissement des vibrations de tôles par revêtement*, ed. H. Mynche. 1–10. G.A.L.F. Leuven 14–19, September 1967.
2. Kerwin Jr., E. M., Damping of flexural waves by a constrained viscoelastic layer. *J. Acoust. Soc. Am.*, **31** (1959) 952–62.
3. Kerwin, Jr., E. M., Macromechanism of damping in composite structures. In *67th Annual Meeting of ASTM*, Chicago (1964) pp. 125–49.
4. Nakra, B. C., Vibration control with viscoelastic materials. *Shock and Vibration Digest* (1976) 3–12.
5. Mead, D. J. & Pearce, T. G., The optimum use of unconstrained layer damping treatments. A.A.S.U. Report 126, University of Southampton (1962).
6. Mead, D. J., The optimum use of unconstrained layer damping treatment. Wright Patterson Air Force Base, Ohio, Technical DOC. No. AFML-TDR-64-51 (1964).
7. Lunden, R., Optimum distribution of additive damping for vibrating beams. *J. Sound. and Vib.*, **66** (1979) 25–37.
8. Baumgarten, J. R. & Pearce, B. K., The damping effects of viscoelastic materials. Part 1—Transverse vibrations of beams with viscoelastic coatings. *Journal of Engineering for Industry* (1971) 645–50.
9. Miles, R. N. & Reinhall, P. G., An analytical model for the vibration of laminated beams including the effects of both shear and thickness deformation in the adhesive layer. *ASME Journal of Vibration, Acoustics, Stress, Reliability and Design*, **108** (1981) 56–64.
10. Rao, M. D. & He, S., Dynamic analysis and design of laminated composite beams with multiple damping layers. *AIAA Journal*, **31** (1993) 736–45.
11. Parthasarathy, P., Partial coverage of rectangular plates by unconstrained layer damping treatments. *J. of Sound. and Vib.*, **102** (1985) 203–16.
12. Parthasarathy, P., Study of unconstrained layer damping treatment applied to rectangular plates having central cutouts. *Computers and Structures*, **23** (1986) 433–43.
13. Corsaro, R. D. & Sperling, L. H., *Sound and Vibrations with Damping with Polymers*. American Chemical Society, Washington D.C. (1990) 470 pp.
14. Alberts, T. E., Xia, H. & Chen, Y., Dynamic scaling of flexible structures with viscoelastic components. *Journal of Vibrations and Acoustics*, **114** (1992) 449–53.
15. Hajela, P. & Lin, C. Y., Optimal design of viscoelastically damped beam structures. *Appl. Mech. Rev.*, **44** (1991) S96–S106.
16. Sun, C. T., Sankar, B. V. & Rao, V. S., Damping and vibration control of unidirectional composites laminates using add-on viscoelastic material. *J. of Sound and Vib.*, **139** (1990) 277–87.
17. Cheng, L. & Nicolas, J., Radiation of sound into a cylindrical enclosure from a point-driven end plate with general boundary conditions. *J. Acoust. Soc. Am.*, **91**(3) (1992) 1504–13.
18. Cheng, L. & Richard, M., A new formulation for the vibration analysis of a cylindrical vessel containing fluid via the use of artificial spring systems. *Thin-Walled Structures*, **21** (1995) 17–30.

19. Nashif, A. D. & Lewis, T. M., Data base of the dynamic properties of materials. *Sound and Vibration* (1991) 14–25.
20. Drake, M. L., Section 7.1 – Fourth-Order Beam Theory. Vibration Damping Short Course Notes, University of Dayton Research Institute.
21. Press, W. H., Teukolsky, S. A., Vetterling, W. T. & Flannery, B. P., *Numerical Recipes in FORTRAN*, 2nd edn. Cambridge University Press, UK (1992) 963 pp.

APPENDIX 1

Formulas for $[M]$, $[K]$, and $[F]$

$$M_{pqrs} = M_{pqrs}^{plate} + M_{pqrs}^{visco}$$

$$M_{pqrs}^{plate} = \begin{cases} \frac{8\rho_p b h e}{(p+r+1)(q+s+1)} & \left(\begin{array}{l} \text{for } (p+r) \text{ and} \\ (q+s) \text{ even} \end{array} \right) \\ 0 & \text{(otherwise)} \end{cases}$$

$$M_{pqrs}^{visco} = \sum_{i=1}^X \sum_{j=1}^Y c(i, j) \{ 2\rho_v e_v b h [(-X+2i)^{p+r+1} - (-X+2(i-1))^{p+r+1}] \\ \times [(-Y+2j)^{q+s+1} - (-Y+2(j-1))^{q+s+1}] \} \\ / (p+r+1)(q+s+1) X^{p+r+1} Y^{q+s+1}$$

$$K_{pqrs} = K_{pqrs}^{plate} + K_{pqrs}^{visco} + K_{pqrs}^{edges}$$

$$K_{pqrs}^{plate} = \begin{cases} \frac{8E_p e^3}{3(1-\nu_p^2)} \\ \times \left[\frac{hpr(p-1)(r-1)}{b^3(p+r-3)(q+s+1)} + \frac{bqs(q-1)(s-1)}{h^3(q+s-3)(p+r+1)} + \right. \\ \left. \frac{\nu_p[qr(q-1)(r-1) + ps(p-1)(s-1)] + 2(1-\nu_p)pqrs}{bh(p+r-1)(q+s-1)} \right] \\ 0 & \left(\begin{array}{l} \text{for } (p+r) \text{ and} \\ (q+s) \text{ even} \end{array} \right) \\ \text{(otherwise)} \end{cases}$$

$$K_{pqrs}^{visco} = \sum_{i=1}^X \sum_{j=1}^Y c(i, j) \frac{2E_v(3e^2 e_v + 3ee_v^2 + e_v^3)}{3(1-\nu_v^2)}$$

$$\begin{aligned}
 & \times \left\{ \frac{hpr(p-1)(r-1) \left\{ [(-X+2i)^{p+r-3} - (-X+2(i-1))^{p+r-3}] \right\}}{b^3(p+r-3)(q+s+1)X^{p+r-3}Y^{q+s+1}} \right. \\
 & + \frac{bqs(q-1)(s-1) \left\{ [(-X+2i)^{p+r+1} - (-X+2(i-1))^{p+r+1}] \right\}}{h^3(p+r+1)(q+s-3)X^{p+r+1}Y^{q+s-3}} \\
 & \left. + \frac{\left[v_v \left[\begin{matrix} qr(q-1)(r-1) \\ +ps(p-1)(s-1) \\ +2(1-v_v)pqrs \end{matrix} \right] \left\{ [(-X+2i)^{p+r-1} - (-X+2(i-1))^{p+r-1}] \right\}}{bh(p+r-1)(q+s-1)X^{p+r-1}Y^{q+s-1}} \right\} \right. \\
 K_{pqrs}^{edges} &= 2 \left[\frac{h \left[(-1)^{p+r} k_1 + k_2 + \frac{pr}{b^2} ((-1)^{p+r-2} c_1 + c_2) \right]}{q+s+1} \right. \\
 & \left. + \frac{b \left[(-1)^{q+s} k_3 + k_4 + \frac{qs}{h^2} ((-1)^{q+s-2} c_3 + c_4) \right]}{p+r+1} \right]
 \end{aligned}$$

*Note: k_1 and c_1 : edge x (-) k_2 and c_2 : edge x (+)
 k_3 and c_3 : edge y (-) k_4 and c_4 : edge y (+)

$$F_{pq} = \sum_{\delta=1}^{\Delta} F_{\delta} \left(\frac{x_{\delta}}{b} \right)^p \left(\frac{y_{\delta}}{h} \right)^q$$

**Note: This formulation for F_{pq} is valid only for sinusoidal concentrated loads of amplitude F_{δ} at (x_{δ}, y_{δ}) .

APPENDIX 2

Properties of the viscoelastic material

| <i>Soundcoat D</i> (Material parameters) | |
|---|--------|
| Density (kg/m ³) | 970 |
| T_0 (°C) | 120 |
| FROM | 1.00E4 |
| MROM (N/m ²) | 9.11E5 |
| N | 0.204 |
| ML (N/m ²) | 1.64E3 |
| ETAFROL | 0.800 |
| S _L | 0.300 |
| S _H | -0.220 |
| FROL | 1.64E3 |
| C | 5.00 |

$$\log(FR) = \log(F) - \frac{12(T - T_0)}{291.66 + T - T_0}$$

$$A = \frac{1}{C} \left[\log \left(\frac{FR}{FROL} \right) \right]$$

$$\log(\gamma_v) = \log(ETAFROL) + \left(\frac{C}{2} \right) \left[\frac{(S_L + S_H)A +}{(S_L - S_H)(1 - \sqrt{1 + A^2})} \right]$$

$$\log(G_v^*) = \log(ML) + \frac{2 \log(MROM/ML)}{[1 + (FROM/FR)^N]}$$

$$E_v^* = G_v^* \times 2(1 + v_v) \quad E_v = E_v^*(1 + j\gamma_v)$$